SOVIET PHYSICS USPEKHI VOLUME 14, NUMBER 4 JANUARY-FEBRUARY, 1972

537.311.33

INFLUENCE OF PRESSURE ON THE FERMI SURFACE OF METALS

N. B. BRANDT, E. S. ITSKEVICH, and N. Ya. MININA

Moscow State University; Institute of High-pressure Physics, USSR Academy of Sciences

Usp. Fiz. Nauk 104, 459–488 (July, 1971)

CONTENTS

1. INTRODUCTION

THE last decade has been characterized by intense development of theoretical and experimental research on the energy spectra of electrons in metals. The most general characteristic of the energy spectrum is the Fermi surface of constant energy $\mathcal{E}(\mathbf{k}) = \mathcal{E}_F$ ($\mathcal{E}_F$—Fermi energy, $\mathbf{k}$—wave vector), which separates the occupied electronic states from the free ones in momentum space. The shape of the Fermi surface, which in the general case can be very complicated, and also the main characteristics of the electrons with Fermi energy, determine practically all the electronic properties of metals.

The experimental study of the energy spectra is carried out principally by observing effects due to the quantization of the electron energy in a constant magnetic field (Landau quantization). These experiments yield directly such important parameters as the areas of the extremal sections of the Fermi surface (the de Haas–van Alphen and Shubnikov–de Haas effects), the effective carrier masses (cyclotron resonance), and others.

Besides quantum effects, certain information concerning the electronic energy spectrum is obtained by investigating the galvanomagnetic characteristics of metals in strong magnetic fields (information on the topology of the Fermi surface) and of semimetals in weak magnetic fields.

The energy spectrum of the electrons in a metal is determined not only by the properties of the ions forming the crystal lattice, but also by their mutual placement and by the distances between them. Theoretical models of the spectrum are usually compared with the experimental data obtained at equilibrium values of the lattice parameters. Investigations under pressure make it possible to trace the character of the change in the main parameters of the spectrum (in particular, the shape of the Fermi surface) in a definite interval of the values of the lattice constant, and thus uncover new possibilities for experimental verification of different theoretical models.

As is well known, the principal role in the formation of the electron spectrum is played by the periodic lattice potential. At the present time, the most widely used method of taking this potential into account in the theoretical determination of the spectrum is the pseudopotential method, in which the conduction electrons are assumed to be almost free, and the effective potential acting on them (the pseudopotential) is regarded as a perturbation. The feasibility of such a consideration is based on the fact that the conduction electrons experience effective repulsion from the ions, since their wave functions are orthogonal to the wave functions of the internal shells of the ions. This repulsion cancels almost completely the large Coulomb potential of the latter and causes the pseudopotential to be small compared with the energy of the Fermi electrons.

The indicated feature of formation of the pseudopotential is the reason why it can experience appreciable changes under the influence of pressure. The use of pressure as a continuous (thermodynamic) parameter of the system makes it possible to verify theoretical conclusions having a broader meaning. An example is the experimental verification of Kane's law that the electron effective mass is proportional to the width of the gap in the energy spectrum of narrow-gap semiconductors[1], or the experimental confirmation of the Geĭlikman and Kresin theory[2] of superconductors with strong coupling.

Besides the study of the quantitative changes of the spectrum under pressure, great interest attaches to changes in which the spectrum is qualitatively altered. Many situations can arise in this case: a transition of a metal into the dielectric state, owing to the vanishing of the overlap between the valence band and the conduction band and the vanishing of the volume of all parts of the Fermi surface; a change in the topology of the Fermi surface, wherein individual parts of the surface break away or vanish, the conductivity is changed, etc. Such "electronic" phase transitions, predicted by Lifshitz[3], have by now been observed in a number of metals.

Recently interest in the investigation of electronic energy spectra of metals at high pressures has greatly increased, owing, on the one hand, to the development of new experimental and theoretical methods of investigating the spectrum, and on the other hand to the appreciable progress in the development of special apparatus for producing high pressures at low temperatures.

In the present review we do not treat the theory of effects investigated for the study of energy spectra of carriers in metals. These questions have been the subject of a sufficient number of special reviews (see, for example, the review of Lifshitz and Kaganov[4]).

Principal attention will be paid by us to the presently known data on the changes occurring in the Fermi surfaces of metals under pressure and to a description of methods of producing hydrostatic pressures at low temperatures.

Insofar as we know, there is at present no review devoted to this topic and covering in sufficient detail the entire available experimental material*.

2. METHODS OF OBTAINING HIGH PRESSURES FOR THE STUDY OF THE ENERGY SPECTRUM OF METALS

Modern methods of investigating the energy spectrum of metals require simultaneous use of low temperatures, sufficiently strong and homogeneous magnetic fields, and a high degree of perfection of the investigated crystals. These conditions impose definite requirements on the apparatus used to obtain high pressures. It is obvious that the employed chambers must be sufficiently small and autonomous, they should be made of nonmagnetic materials, and the pressures obtained in them should be hydrostatic to a good degree.

All the methods for producing hydrostatic pressures at low temperatures encounter one principal difficulty—the absence at these temperatures of a sufficiently plastic medium for transferring the pressure to the sample. Ideal hydrostatic conditions are obtained only by the compression of liquid helium, but the maximum pressures that can be obtained by this method are very low (on the order of 100 bar).

In 1960, Balain et al. were the first to use hydrostatic pressure produced by liquid helium to investigate oscillatory effects in zinc, in which the pressure effect turned out to be considerable[6].

The low value of the pressure obtained in this manner has delayed for a long time the investigations of other metals. In 1965, Templeton turned to the use of liquid helium to produce pressure[7]. He employed a sensitive procedure for recording the changes, under pressure, of the oscillation frequency in the de Haas—van Alphen effect by determining the phase shift (Shoenberg et al.[8]). The change of the oscillation phase makes it possible to calculate the derivative of the corresponding section of the Fermi surface with respect to pressure.

Structurally, the apparatus of Balain et al. and of Templeton consisted of a bomb made of a nonmagnetic material, connected by a capillary to a cylinder containing helium gas.

In research on the changes of Fermi surfaces under the influence of pressure, the so-called "fixed-pressure" methods are widely used. The main idea of these methods is that the pressure is produced in the temperature region where the plasticity of the pressure-transmitting media is high enough to ensure hydrostatic compression conditions. The high-pressure chamber is then cooled to the temperature of the experiment. The pressure-transmitting medium then solidifies, and the degree to which the conserved pressure remains hydrostatic is determined principally by the mechanism of solidification and by the change in the volume, and consequently by the pressure loss incurred during the solidification and subsequent cooling. The lower the solidification temperature, the smaller is the pressure loss upon solidification and cooling of the medium as a result of thermal compression; in addition, the more "equilibrium" the cooling process, the more hydrostatic is the resultant pressure.

One of the modifications of the "fixed pressure" method is the "ice procedure" developed in 1944 by Lazarev and Kan[9], in which pressure is produced by expansion of water that freezes in a closed vessel. The maximum pressure obtained in this method is about 2 kbar. A shortcoming of the "ice procedure" is the strong adhesion of the ice to the surface of the sample, as a result of which considerable inhomogeneous stresses can arise upon freezing. The use of a medium that is more plastic (in the solidification region), namely a water-alcohol solution[10], improves the situation somewhat and also makes it possible to vary the pressure by varying the alcohol concentration in the solution.

The second method of obtaining a "fixed pressure," which was used to initiate research on oscillatory effects and the angular dependence of the magnetoresistance at pressures above 2 kbar, was developed by Itskevich and co-workers in 1962[11,12]. A pressure up to 18 kbar is produced with the aid of a hydraulic press at room temperature in an autonomous piston chamber in a hydrostatic medium—a mixture of kerosene with oil. The pressure is then mechanically fixed, and the chamber is slowly cooled to liquid-helium temperature. Upon cooling, the pressure decreases by approximately 3 kbar as a result of the difference between the thermal-expansion coefficients of the material and the contents of the chamber. The chamber is made of nonmagnetic materials, mainly of heat-treated beryllium bronze, which makes it possible to work with strong magnetic fields. The sufficiently high plasticity of the medium during the course of solidification and the relatively small loss of pressure upon solidification and cooling ensure that the inhomogeneous stresses in the sample are low.

Figure 1 shows one chamber of this type, used at the present time for the investigation of quantum effects under pressure. We call attention to the fact that the use of an obturator with electric leads sealed with epoxy resin[13] greatly facilitates the mounting of the samples and the practical utilization of the chamber. The pressure is measured at the temperature of the experiment with manganin resistance manometers and with superconductor manometers based on the pressure depen-

*A recently published article by Dugdale "Some Aspects of High Pressures at Low Temperatures" [5] considered only individual aspects of this problem.

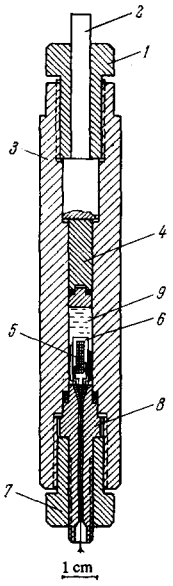

FIG. 1. Chamber for producing hydrostatic pressures up to 16 kbar with kerosene-oil medium. 1–Nut, 2–rod to transmit the force from the press, 3–body of bomb, 4–working piston with mushroom packing, 5–sample, 6–sample holder, 7–stopping nut of obturator, 8–obturator, 9–pressure-transmitting medium.

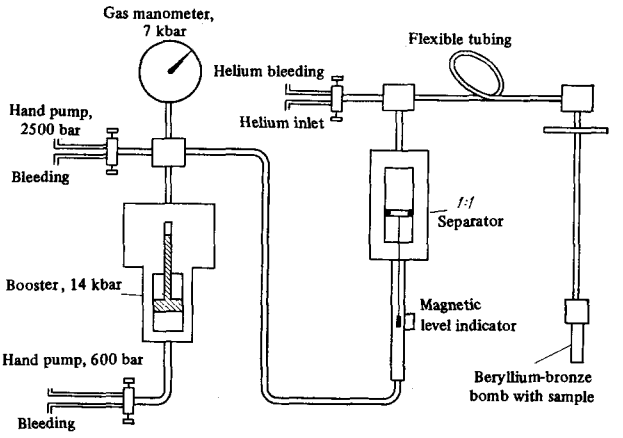

FIG. 3. Setup for obtaining hydrostatic pressure with the aid of solid helium.

dence of the temperature of transition into the superconducting state. The use of superconducting manometers, which record the superconducting transition by a contactless method, offers definite convenience in operation (see, for example,[14]).

In 1968–1969, the procedure of[11] was modified (Fig. 2) by Brandt, Minina, and Ponomarev[15-16]. A special design of the pistons and of their packings has made it possible to raise the pressure to 20–22 kbar, and the use of a pentane-oil mixture as the pressure-transmitting medium made the pressure highly hydrostatic.

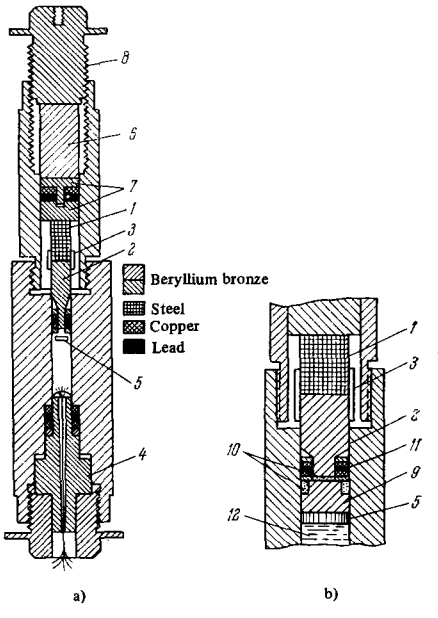

FIG. 2. Chamber for hydrostatic pressures up to 22 kbar with pentane-oil medium. a) Overall view of bomb: 1, 2–composite piston in high-pressure chamber, 3–cambric sleeve, 4–obturator with inlets for samples, 5–tin manometer, 6–cylinder of heat-treated beryllium bronze, transmitting the force to the piston, 7–piston in low-pressure chamber, 8–stopping nut (the pressure is produced by screwing in the nut 8). b) Cylinder packing used when working with pentane-oil mixture: 9–beryllium bronze button, 10–oil cushion, 11–gaskets, 12–pentane-oil mixture in high-pressure chamber.

In 1965, to investigate the influence of pressure on quantum oscillations of the magnetoresistance, Schirber[17] successfully employed a procedure developed by Swenson et al.[18] for producing sufficiently hydrostatic pressures (up to 7 kbar) by isobariz freezing of compressed helium*.

The apparatus (Fig. 3) consists of helium and air high-pressure systems. The helium part consists of the chamber with the sample, connected through a capillary to a system for preliminary filling with helium and a separator for producing the working pressure. The air pressure is produced in the separator by a booster with the aid of two pumps. The necessary pressure is produced in the chamber at a temperature above the melting point of helium and is maintained constant while the chamber is gradually cooled. The pressure of the gaseous phase is determined with the aid of a gas manometer. The correction for the temperature change is calculated from the isochores of solid helium. The decrease of the pressure in the chamber when cooled to liquid-helium temperature is 10%.

Chambers with liquid mixtures[11,15] have many advantages over setups using compressed helium. They make it possible to obtain much higher pressures, are simpler to construct, and it is easier to generate the pressure in them and to perform the experiments. The autonomy of the chambers affords greater possibilities for their use. Finally, we note the reliability and relative safety of operating with hydraulic chambers as compared with gas chambers.

Chambers with liquid mixtures were used to investigate the oscillatory effects under pressure in Zn and in semimetals (Bi, Sb, graphite). Chambers using solid helium were used to study a number of metals (Zn, Pb, Al, In, Cd, Be) and semimetals (Sb and graphite). The data obtained by both methods practically coincide,

*In the first variant of this procedure, the cooling was carried out at constant value [19].

although, to be sure, agreement for Zn is obtained only at pressures above 2—3 kbar.

The foregoing methods for obtaining high pressures at low temperatures constituted a great step forward, since the degree to which the compression was hydrostatic in them turned out to be sufficient for the investigation of quantum oscillatory effects under pressure, thereby affording a possibility for obtaining direct information on the character of the variation of the energy spectrum of metals when the lattice parameters are varied.

3. INFLUENCE OF CRYSTAL-LATTICE PARAMETERS ON THE ENERGY SPECTRUM OF THE ELECTRONS IN A METAL FROM THE POINT OF VIEW OF THE CONCEPTS OF THE PSEUDOPOTENTIAL AND THE ALMOST-FREE-ELECTRON MODEL

We consider first very briefly the main ideas and the procedure for constructing Fermi surfaces by the pseudopotential method.

When an electron is scattered in a crystal lattice, the initial wave vector **k** is changed by a certain vector **q**, so that in the state after the scattering the wave vector takes on the value **k** + **q**. The probability of such a scattering is determined by the matrix element of the pseudopotential W, which can be represented in the form[20]

$$\langle \mathbf{k}|W|\mathbf{k}+\mathbf{q}\rangle = S(\mathbf{q})\langle \mathbf{k}|w|\mathbf{k}+\mathbf{q}\rangle, \tag{1}$$

where

$$S(\mathbf{q}) = \frac{1}{N}\sum_j e^{-i\mathbf{q}\mathbf{r}_j} \tag{2}$$

($\mathbf{r}_j$ are the radius vectors determining the positions of the ions in the metal),

$$\langle \mathbf{k}|w|\mathbf{k}+\mathbf{q}\rangle = \frac{1}{\Omega}\int e^{-i\mathbf{k}\mathbf{r}} w(r)\, e^{i(\mathbf{k}+\mathbf{q})\mathbf{r}}\, d\tau \tag{3}$$

(Ω is the atomic volume).

It follows from (1)—(3) that the matrix element of the pseudopotential is a product of two independent quantities, the structure factor S(q) determined only by crystal geometry, and the form factor $\langle \mathbf{k}|w|\mathbf{k}+\mathbf{q}\rangle$, which depends on the chemical nature of the ions (w is the pseudopotential of the individual ion).

It can be shown that the structure factor S(q) differs from zero only for vectors **q** belonging to the reciprocal lattice. Therefore for the states of an electron with wave vector **k** lying on one of the faces of the Brillouin zone the only possible states after scattering are states with wave vector **k** + **q**. In this connection, the states of the electron near the faces of the Brillouin zone are described by two orthogonalized plane waves (2-OPW), corresponding to the vectors **k** and **k** + **q**.

If the vector **k** belongs simultaneously to two faces whose defining vectors are $\mathbf{q}_1$ and $\mathbf{q}_2$, i.e., it lies on an edge of the Brillouin zone, then the electron in such a state will experience effective scattering from two planes. Therefore the state of the electron near the edges of the zone is described by three OPW, corresponding to the vectors **k**, **k** + $\mathbf{q}_1$, and **k** + $\mathbf{q}_2$.

In analogy, to describe states lying at corners of the zone, where three faces intersect, the 4-OPW approximation is used.

The problem of constructing the Fermi surface consists mathematically of determining the eigenvalues of the conduction-electron energy. For states sufficiently remote from the faces of the Brillouin zone, perturbation theory is used. Usually the analysis is confined to second order in the matrix elements of the pseudopotential. The expression for the energy is

$$\mathscr{E}(\mathbf{k}) = \frac{\hbar^2}{2m}(\mathbf{k})^2 + \langle \mathbf{k}|W|\mathbf{k}\rangle + \sum_{\mathbf{q}\neq 0}\frac{\langle \mathbf{k}+\mathbf{q}|W|\mathbf{k}\rangle\langle \mathbf{k}|W|\mathbf{k}+\mathbf{q}\rangle}{(\hbar^2/2m)[\mathbf{k}^2-(\mathbf{k}+\mathbf{q})^2]}. \tag{4}$$

The first term in (4) is the free-electron energy and corresponds to the solution of the problem in the one-wave approximation (1-OPW), which is also called the almost-free-electron approximation. The second determines the correction of first order in the pseudopotential, the third the second-order correction, etc.

Formula (4) makes it possible in principle to construct the Fermi surface $\mathscr{E}(\mathbf{k}) = \mathscr{E}_F$ if one knows the matrix elements of the pseudopotential. We note that an essential circumstance in this case is the condition that the energy denominators in (4) do not vanish. This condition is satisfied for states not lying on the faces of the Brillouin zone.

When the wave vector **k** of the initial state lies on a face of the Brillouin zone, then the perturbation-theory series diverges. The wave function of such states, as indicated, is described in the 2-OPW approximation. Substitution of the corresponding wave function into the Schrödinger equation leads to a secular equation that determines the eigenvalues of the energy E:

$$\left(\frac{\hbar^2}{2m}\mathbf{k}^2 - E\right)\left(\frac{\hbar^2}{2m}(\mathbf{k}+\mathbf{q})^2 - E\right) - |W_{\mathbf{q}}|^2 = 0; \tag{5}$$

Here $|W_{\mathbf{q}}|^2$ is the square of the modulus of the matrix element of the pseudopotential. The solution of (5) makes it possible to find the dependence of the energy E on the wave vector **k**, and by the same token to construct the Fermi surface in the immediate vicinity of the faces of the Brillouin zone.

For the state of an electron whose wave vector lies on an edge of the Brillouin zone or at a vertex, the corresponding secular equation will be of third or fourth degree in the energy E.

Thus, the general approach to the construction of the Fermi surface within the framework of the pseudopotential theory reduces to the following. The surface is first constructed with the aid of the Fermi spheres

$$\mathscr{E}(\mathbf{k}) = \frac{\hbar^2}{2m}(\mathbf{k}_F - \mathbf{q})^2, \tag{6}$$

with centers at different reciprocal-lattice points. The segments of the spheres cut off by the faces of the Brillouin zone, form parts of the Fermi surface, which belong in accordance with definite rules to one zone or another (the 1-OPW approximation). Then, for states on this sphere which are sufficiently remote from the faces of the Brillouin zone, one calculates the corrections by perturbation theory, while for states near the faces of the zone the calculation is carried out in the corresponding wave approximation using the secular equations.

The equations obtained as a result of the calculation for the Fermi surface contain matrix elements of the pseudopotential, the values of which can be obtained by

comparison with experiment. Methods of theoretical calculation of the matrix elements have been the subject of an extensive literature (see, for example,[20]). For our purposes, however, sufficiently simple methods (the so-called model potentials) suffice. In the analysis of the experimental data on the influence of pressure on the Fermi surface, we shall regard the matrix elements as specified functions of the parameter q/k_F.

The radius k_F of the Harrison sphere is defined by the expression

$$k_F = \left(\frac{3\pi^2 Z}{\Omega}\right)^{1/3}, \quad (7)$$

where Z is the number of valence electrons. In spite of its approximate character, the single-wave approximation has the advantage that, by relating the dimensions of the Fermi surface with the parameters of the crystal lattice, it provides a simple and fully defined description of the change occurring in the Fermi surface as a whole under pressure. Under hydrostatic compression, the atomic volume Ω decreases and the volumes of the Fermi sphere and of the Brillouin zone increase. Here, naturally, changes also take place in the areas of the sections of the Fermi surface. In the almost-free-electron model (AFEM) in the case of isotropic compressibility, the relative change under pressure of the sections S_F of the Fermi surface should be proportional to the volume compressibility of the metal:

$$\frac{\Delta S_F}{S_F} = -\frac{2}{3}\frac{\Delta\Omega}{\Omega}, \quad (8)$$

i.e., the shapes of the individual parts of the Fermi surface remain unchanged, and they grow larger and remain similar to themselves. This follows from the fact that the radius of the Fermi sphere and the dimensions of the Brillouin zone change under pressure in identical manner, i.e., in inverse proportion to the dimensions of the direct lattice. Such a change corresponds, as it were, to a simple increase of the scale in momentum space and at realistically attainable pressures it is, generally speaking, small.

If the crystal lattice changes anisotropically under pressure, then the corresponding anisotropic change in the shape of the Brillouin zone can lead, even in the AFEM, to noticeable changes in the shape of the Fermi surface. Such changes should become manifest particularly strongly in metals possessing high compressibility anisotropy. An estimate of such changes can be made with the aid of the suitable Harrison construction for the compressed metal, if one knows its coefficients of linear compressibility.

The character of the compression-induced change of the parts of the Fermi surface lying near the faces of the Brillouin zone is not described by the AFEM and is directly connected with the change under pressure of the matrix elements of the pseudopotential, since their role in the formation of the spectrum near the faces is usually decisive.

Thus, in the general case the change of the Fermi surface of metals under the influence of pressure is determined by two factors: the change of the geometry (parameters) of the crystal lattice, and the change of the magnitude (and perhaps also the sign) of the matrix elements of the pseudopotential.

4. CHANGE OF THE FERMI SURFACES OF METALS UNDER HYDROSTATIC COMPRESSION

At the present time, the influence of pressure on the Fermi surface has been investigated for a large number of metals with different crystal lattices, which can be classified as follows:

1. Metals with face-centered cubic lattice—copper, silver, gold, lead, potassium, rubidium, cesium, palladium, platinum, aluminum.
2. Metals with tetragonal lattice—indium.
3. Metals with hexagonal close-packed lattice—zinc, cadmium, beryllium, thallium.
4. Semimetals with rhombohedral structure—bismuth, antimony, arsenic, and with layered lattice—graphite.

In view of the complexity of the problem, these researches are far from complete, and concern in most cases small sections of the Fermi surface, which are most sensitive to the deformation of the crystal.

In accordance with the changes of the lattice parameters upon compression, the metals in question are divided into two groups. The first includes cubic metals having almost isotropic compressibility, such as Cu, Ag, Au, and Pb, and the other, conversely, includes metals that are strongly anisotropic: Zn, Cd, graphite.

5. METALS WITH CUBIC LATTICE

5.1. Noble Metals: Copper, Silver, Gold

The influence of pressure on the Fermi surface of noble metals was investigated by the phase-shift method by Templeton[7] and by Sullivan and Schirber[21]. A pressure up to 25 bar was produced with the aid of liquid helium.

The multiply-connected electronic Fermi surface of copper (Fig. 4), just like the equal-energy surfaces of gold and silver, consists of a number of spheres with centers at the points Γ of the Brillouin zones, interconnected in directions of the [111] types by thin bridges—"necks"—which were formed as a result of the perturbing action of the Brillouin-zone boundaries.

Templeton measured the pressure-induced changes of the sections of the "sphere" $d(\ln S_1)/dp$ and of the "neck" $d(\ln S_2)/dp$ perpendicular to the [111] direction,

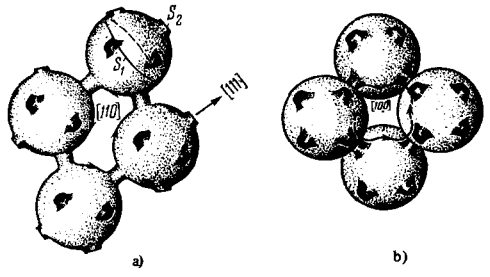

FIG. 4. Fermi surface of copper, gold, and silver. In the [110] direction (a) there are observed "dog-bone" hole orbits. In the [100] direction (b) one observes hole orbits having the form of a fourth-order "rosette" and passing over the upper and lower sides of the spheres with centers in different planes.

Table I

Determined quantity	Direction of magnetic field	Cu[7,21,22]	Ag[7]	Au[7]
Volume Compressibility $\left(\frac{d\ln\Omega}{dp}=\frac{1}{\Omega}\frac{\Delta\Omega}{\Delta p}\right)$		−0.6907	−0.9023	−0.544
Increase of Fermi-surface cross section in accord with the AFEM $\frac{d\ln S_F}{dp}$		0.4605	0.6015	0.3627
Observed "change" of the "sphere" cross section $\frac{d\ln S_1}{dp}$	[111]	0.421 [7] 0.425 [21] 0.435 [22] (theor.)	0.503	0.284
$\frac{d\ln S_1}{d\ln S_F}$		0.97 [7]	0.83	0.78
$\frac{d\ln S_1}{dp}$	[100]	0.46 [21] 0.462 [22] (theor.)		
Distortion of "sphere" $\left(\frac{d\ln S_1}{dp}-\frac{d\ln S_F}{dp}\right)$	[111]	−0.04 [7]	−0.099	−0.079
Change of "neck" cross section $\frac{d\ln S_2}{dp}$	[111]	1.93 [7] 1.8 [21] 1.53 [22] (theor.)	4.40	1.97
$\frac{d\ln S_2}{d\ln S_F}$		4.2 [7]	7.3	5.4
Distortion of "neck" $\left(\frac{d\ln S_2}{dp}-\frac{d\ln S_F}{dp}\right)$	[111]	1.47 [7]	3.8	1.61
Change of area of the "dog-bone" orbit $\frac{d\ln D}{dp}$	[110]	0.4 [21] 0.404 [22] (theor.)		
Change of area of "rosette" orbit $\frac{d\ln R}{dp}$	[100]	0.43 [21]		

All values are given in units of 10^3 kbar^{-1}

and also their relative change $d(\ln S_1)/dp - d(\ln S_2)/dp$, which characterizes the distortion of the Fermi surface.

As expected, an increase was observed in the areas of the central sections of the "necks" S_2 and of the "sphere" S_1 for all three metals (Table I). However, the relative increase of the cross-section areas of the "necks" greatly exceeds the increase of the central sections of the "sphere," although both effects are very small. Therefore, whereas for the sphere a quantitative estimate based on the AFEM describes the experimentally observed changes well (for Cu the interval is $d(\ln S_1)/d(\ln S_F) = 0.91$, where S_F is the cross section of the Fermi sphere), for the "neck" there is an appreciable deviation from this model, namely, the relative change of the "neck" cross section $d(\ln S_2)$ is larger than $d(\ln S_F)$ by 4.2 times for Cu, by 5.4 times for Au, and by 7.3 times for Ag. In other words, the "neck" increases more rapidly than the Fermi sphere of the free electrons, and the spherical part of the surface, conversely, increases more slowly.

A more detailed investigation of the influence of pressure on the Fermi surface of copper, carried out in[21], has shown that the "dog-bone" hole orbits D in the [110] direction and also the quadrangular hole "rosette" R in the [100] direction vary approximately like the sphere (see Table I).

Since the wave functions of the d shells of noble-metal ions are strongly smeared out, the pseudopotential method is of little use in their study. Davis et al. calculated the band structure of copper as a function of the crystal-lattice parameters by the Corringa-Kohn-Rostoker method[22]. Good agreement was obtained between the experimental and theoretical data (see Table I)*.

5.2. Lead

In view of the fact that the number of valence electrons in lead is equal to four, its Fermi surface is much more complicated and its parts are disposed in several energy bands.

*Analogous calculations were carried out also by Schirber and O'Sullivan for copper, gold, and silver (Colloq. Int. CNRS 188, 113 (1970)).

Anderson et al.[23] used the procedures of[17] and[7] to measure the de Haas–van Alphen effect in lead under pressure. The measurements, in which a pressure up to 4–5 kbar was produced with the aid of solid helium, showed that under the influence of pressure the cross-section areas ψ of the hole part of the Fermi surface in the second zone, and also the cross sections ν and ξ of the electron surface in the third zone (Fig. 5) increase by $\sim 0.3\%$ kbar^{-1}. Approximately the same changes were obtained for the cross sections ψ and ξ by the phase-shift method using liquid helium to produce the pressure. The obtained values are almost double the values corresponding to the AFEM.

To calculate the change of the matrix elements under pressure, the analytical expression obtained by Anderson and Gold[24] by the pseudopotential method in the 4-OPW approximation was used for the cross section of the Fermi surface. In the general form, the cross section can be expressed in the following manner:

$$S = \left(\frac{2\pi}{a}\right)^2 S_0(\mathcal{E}_F, W_{111}, W_{200}, \lambda), \tag{9}$$

where S_0 is the cross section in dimensionless units, W_{111} and W_{200} are the matrix elements of the pseudopotential that mix states differing by the reciprocal-lattice vectors $(2\pi/a)[111]$ and $(2\pi/a)[200]$, respectively, and λ is a parameter that takes the spin-orbit interaction into account. The relative change under pressure is

$$\frac{1}{S}\frac{dS}{dp} = -\frac{2}{3}\frac{1}{\Omega}\frac{d\Omega}{dp} + \frac{1}{S_0} \tag{10}$$
$$\left(\frac{\partial S_0}{\partial \mathcal{E}_F}\frac{\partial \mathcal{E}_F}{\partial p} + \frac{\partial S_0}{\partial W_{111}}\frac{\partial W_{111}}{\partial p} + \frac{\partial S_0}{\partial W_{200}}\frac{\partial W_{200}}{\partial p} + \frac{\partial S_0}{\partial \lambda}\frac{\partial \lambda}{\partial p}\right).$$

It is obvious that the quantity $(2/3\Omega)(d\Omega/dp)$, which is determined by the compressibility, describes only in part the change of the real cross section of the Fermi surface, an appreciable contribution to which is made by the second term on the right, which is connected with the pressure dependence of $\mathcal{E}_F$ and of the matrix elements W_{111} and W_{200} (λ is assumed to depend little on the pressure).

With the aid of expressions (9) and (10) and the experimental data on the change of the different cross sections under pressure, the following values were obtained for the parameters in (10):

$$\frac{1}{\mathcal{E}_F}\frac{\partial \mathcal{E}_F}{\partial p} \approx -0.044\cdot 10^{-2} \text{ kbar}^{-1},$$
$$\frac{1}{W_{111}}\frac{\partial W_{111}}{\partial p} \approx -0.58\cdot 10^{-2} \text{ kbar}^{-1},$$
$$\frac{1}{W_{200}}\frac{\partial W_{200}}{\partial p} \approx -1.8\cdot 10^{-2} \text{ kbar}^{-1},$$

where in accord with[23] $W_{111} = -0.084$, $W_{200} = -0.39$, and $\mathcal{E}_F = 0.178$ rydberg.

A theoretical estimate of the change of the matrix elements was carried out with the aid of a model potential of a pointlike ion[20]:

$$V_M = S(\mathbf{q})\langle \mathbf{k}|w|\mathbf{k}+\mathbf{q}\rangle = S(\mathbf{q})[(-4\pi e^2/q^2)+\beta][\Omega\varepsilon(q)]^{-1}, \tag{11}$$

where $\epsilon(q)$ is the dielectric constant and β is a parameter characterizing the repulsion of the conduction electrons by the internal ion shells. The calculated values turned out to be smaller by a factor of 4–5 than those determined experimentally, although they agree

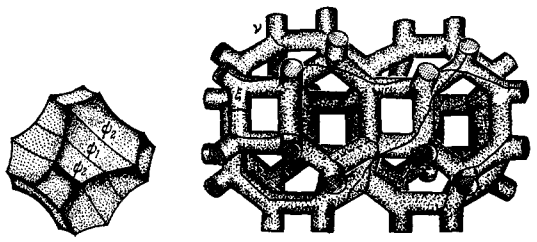

FIG. 5. Hole (left) and electron parts of the Fermi surface of lead in the second and third zones, respectively [24].

in sign. This discrepancy shows that the parameter β in (11) depends on the pressure, but with a very large value $(1/\beta)(\partial\beta/\partial p) = 3\times 10^{-2}$ kbar^{-1}. An analogous disparity between the model of the pointlike ion and experiment is observed also for Zn, and its cause, in all probability, is the inaccuracy in the determination of the model potential.

5.3. Alkali Metals: Potassium, Rubidium, Cesium

The influence of pressure on the Fermi surface of alkali metals was investigated in two studies.

To obtain exact data on the compressibility of potassium, rubidium and cesium at low temperatures, Templeton and Glinski measured the de Haas–van Alphen effect by the phase-shift method under pressures up to 25 bar at T = 1°K[25].

The Fermi surfaces of these metals lie entirely in the first Brillouin zone, and their shapes differ little from spherical. The areas of the extremal sections S_{extr} of the Fermi surfaces of alkali metals agree well with the results of calculation by formula (7). Their dimensions are smaller than those of noble metals by an approximate factor of 3. The compressibility of alkali metals is anomalously large, and therefore the effect of the change of the Fermi surfaces of alkali metals under pressure is larger than that for noble metals by approximately 50 times.

The results of measurements of the relative change of S_{extr} under pressure are shown in Table II, which also gives the compressibilities calculated from the same data. The Fermi surfaces increase in the volume under pressure, and in the first approximation they apparently remain similar to themselves. The obtained compressibilities are in satisfactory agreement with the previously known experimental data.

Beardsley and Stewart reported in a very brief communication measurements of the angular distribution of the momenta of the photons produced upon annihilation of positrons in rubidium and cesium single crystals under a pressure up to 13 kbar[26]. This distribution

Table II

Metal	$\frac{d\ln S}{dp}$, 10^{-3} kbar^{-1}	Volume compressibility $\varkappa = \frac{d\ln\Omega}{dp}$, 10^{-3} kbar^{-1}
K	17.18±0.08	−25.77±0.13
Rb	21.10±0.1	−31.64±0.15
Cs	26.80±0.13	−40.20±0.2

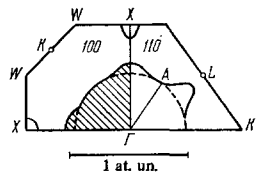

FIG. 6. Intersections of the electron and closed hole parts of the Fermi surfaces of platinum and palladium with the planes (100) and (110) [27].

yields information concerning the part of momentum space filled with electrons in metals, and in the simplest case is suitable for the extraction of information on the Fermi surface. The authors indicate that for rubidium and cesium under a pressure of 13 kbar, the increase of the Fermi surface amounts to 10%. This value was lower by a factor of approximately 2—2.5 than that obtained in the first investigation.

5.4. Transition Metals: Palladium, Platinum

The influence of pressure on the Fermi surface of transition metals—palladium and platinum—was investigated by Vuillemin and Bryant[27], who studied the de Haas—van Alphen effect under pressure up to 25 kbar by the phase-shift method at a temperature below 0.95° K.

In palladium and platinum, as in other transition metals, the Fermi level passes inside a narrow d-band, below its ceiling. The Fermi surface of both metals (Fig. 6), which have a cubic face-centered structure, consists of a closed surface for the s-electrons, lying in the center of the Brillouin zone (point Γ), and two hole surfaces for d holes—three ellipsoids of revolution centered at the points X on quadratic planes of the Brillouin zone, as well as an open surface forming a grid of cylinders elongated along the [100] direction. The electron surface is a sphere on which there are convexities of two sizes: large ones located along the [111] directions, and small ones located along the [100] directions. Owing to the presence of the convexities in the plane perpendicular to the [111] direction, three extremal sections are possible: central, containing the point Γ, and two equivalent noncentral ones.

The authors obtained for both metals the values of the logarithmic derivatives with respect to the pressure, d(lnS)/dp, for the sections of the electronic surfaces perpendicular to the [111] directions (central sections) and to [100]. In Fig. 6, the first section corresponds to the straight line ΓA, and the second to the shaded figure. The derivatives with respect to pressure of both sections are practically identical. $d(\ln S_{[100]})/dp = (0.4 \pm 0.04) \times 10^{-3}$ kbar^{-1} for palladium and $(0.32 \pm 0.03) \times 10^{-3}$ kbar^{-1} for platinum; $d(\ln S_{[111]})/dp = (0.39 \pm 0.04) \times 10^{-3}$ kbar^{-1} and $(0.28 \pm 0.03) \times 10^{-3}$ kbar^{-1}, respectively.

Thus, the pressure leaves the anisotropy of the electron surface almost unchanged.

The obtained broadening of the electron surface exceeds the value calculated by the almost-free-electron model [formula (8)] by 16% for palladium and 30% for platinum.

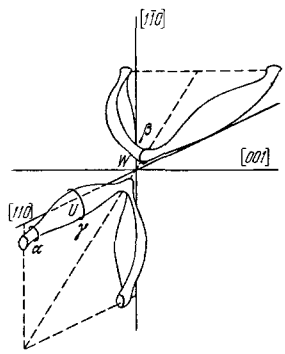

FIG. 7. Sections of the electron equal-energy surface of Al in the third zone. α, β, and γ are different types of extremal sections [28].

5.5. Aluminum

A part of the Fermi surface of aluminum, a trivalent metal with face-centered cubic lattice, investigated under pressure, is shown in Fig. 7. This investigation was carried out by Melz, who used the procedure of[8] to measure the de Haas—van Alphen effect under pressure up to 7 kbar[28]. The investigated part of the Fermi surface consists of quadratic rings lying in the planes of the quadratic faces of the Brillouin zone. Halves of two such rings are shown in Fig. 7. The extremal sections S_β near the corner of the Brillouin zone (the point W) and S_γ with center at the point U at the middle of the edge of the zone were investigated under pressure. It was observed that the cross section S_γ decreases under pressure ($d(\ln S_\gamma)/dp = -4.7 \times 10^{-3}$ kbar^{-1}), whereas according to the AFEM an increase of S_γ should take place with $d(\ln S_\gamma)/dp = 0.74 \times 10^{-3}$ kbar^{-1}. The cross section S_β increases under pressure ($d(\ln S_\beta)/dp = 12 \times 10^{-3}$ kbar^{-1}), in qualitative agreement with the AFEM, but the increase is 16 times faster in magnitude.

Such a strong decrease of S_γ under pressure is due to the singularities of the band structure of Al. In the 3-OPW approximation[29], the energy at the bottom of the third band at the point U is

$$\mathcal{E}_{U_3} = T_U + \frac{1}{2}\{W_{200} + (W_{200}^2 + 8W_{111}^2)^{1/2}\}, \qquad (12)$$

where T_U is the kinetic energy of the free electrons at the point U, while W_{111} and W_{200} are the corresponding matrix elements. The matrix elements W_{111} and W_{200} are positive and, according to Harrison[20], they increase under pressure. This means that the energy $\mathcal{E}_{U_3}$ moves farther away from T_U with increasing pressure, and this effect exceeds the growth of $\mathcal{E}_F$ and T_U under pressure. As a result, the electronic extremum near the point U rises relative to $\mathcal{E}_F$ upon compression, and the Fermi-surface section associated with this extremum decreases.

The use of the model potential of a pointlike ion to estimate the change produced in the matrix elements of the pseudopotential under pressure and the use of expression (12) has made it possible to calculate the change of S_γ:

$$\frac{1}{S_{p=0}}\frac{dS_\gamma}{dp} = \frac{1}{(\mathcal{E}_F - \mathcal{E}_{U_3})_{p=0}}\frac{d(\mathcal{E}_F - \mathcal{E}_{U_3})}{dp}. \qquad (13)$$

The calculated quantity $d(\ln S_\gamma)/dp = -12 \times 10^{-3}$ kbar^{-1} is approximately double the experimental value, but has the correct sign.

5.6. Indium

Indium has a face-centered tetragonal lattice that differs by only 8% from cubic, and has a Fermi surface very similar in shape to the Fermi surface of Al.*

The structure of the electron surface in the third band of indium, the central section of which, S_γ, passes near the point U, is similar to the considered section S_γ of aluminum (see Fig. 7 for aluminum), and is also very sensitive to a change of the lattice potential, since the difference between $\mathcal{E}_F$ and the bottom of the band is comparable with the value of the energy gaps.

An investigation of the dependence of $S_{\gamma'}$ on the pressure in indium, carried out by O'Sullivan and Schirber, who measured the de Haas–van Alphen effect under pressure[30], has shown that it increases at a rate $d(\ln S_{\gamma'})/dp = 7.5 \times 10^{-3}$ kbar^{-1}.

Estimates of the effect with the aid of different form factors reconciled with the experimental data at normal pressure give approximately the same value: d(ln $d(\ln S_{\gamma'})/dp = 6.8 \times 10^{-3}$ kbar^{-1} for the Heine-Abarenkov-Animalu form factor and 7.7×10^{-3} kbar^{-1} for the point-like-ion potential. Since the increase of the cross section due to the change of the lattice parameters is only 3.7×10^{-3} kbar^{-1}, it is obvious that the contribution of the change of the lattice potential accounts for more than one half of $d(\ln S_{\gamma'})/dp$.

The fact that $d(\ln S_\gamma)/dp = -4.7 \times 10^{-3}$ kbar^{-1} for aluminum has the opposite sign is due to the fact that although the form factors of indium, as well as those of aluminum, shift towards increasing energy with increasing pressure, their absolute values, which determine the position of the bottom of the band, decrease for indium (are negative), unlike those of aluminum, and therefore cause a decrease of $\mathcal{E}_{U_3}$ and a corresponding increase of the cross section $S_{\gamma'}$. Figure 8 shows the variation of the form factors of aluminum and indium under pressure.

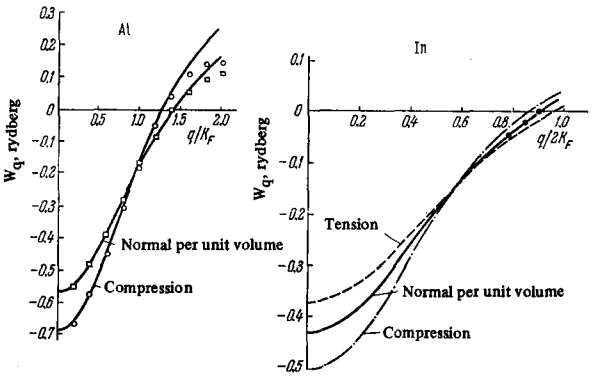

FIG. 8. Form factors of aluminum [20] and indium [30], calculated with the per unit volume in the normal state, compressed, and stretched by 10%.

6. METALS WITH HEXAGONAL CLOSE-PACKED LATTICE

6.1. Zinc, Cadmium

Zinc and cadmium are divalent metals with strong anisotropy of compressibility. Their lattice-parameter ratio c/a exceeds the value 1.633 corresponding to ideal close packing: at T = 4.2°K we have c/a = 1.831 for Zn and 1.863 for Cd. The compressibility anisotropy is characterized by the values $d(\ln c)/dp = -12.07 \times 10^{-4}$ and -18.3×10^{-4} kbar^{-1} and $d(\ln a)/dp = -1.53 \times 10^{-4}$ and -2.1×10^{-4} kbar^{-1} for Zn and Cd, respectively.

A study of these metals under hydrostatic compression is of interest because the strong change of the Brillouin zone due to the compressibility anisotropy can lead to qualitative changes in the topology of the Fermi surface. These changes should be observed primarily in those parts of the Fermi surface which have small volumes.

Figure 9 shows the Fermi surface of Zn, constructed by the AFEM method. It is close to that observed experimentally. For Zn, the radius k_F of the Fermi sphere extends beyond the point K on the edge of the Brillouin zone by less than 1%. The resultant small overlap of the spheres leads to formation of an electron surface in the third band, that has come to be called the "needle." A small change of the parameter ratio c/a or of the carrier density causes a relatively large change of the shape and volume of the "needle."

The sensitivity of the Fermi surface to the ratio c/a can be demonstrated by using as examples Zn, Cd, and Mg, which have the same valence and the same crystal structure. For Mg, c/a = 1.623 and the needle-like surface occupies an appreciable part of the Brillouin zone; for Zn we have c/a = 1.831 and the volume of the "needle" is much smaller ($\sim 10^{-5}$ of the volume of the Brillouin zone); for Cd, c/a = 1.863 and there is no needle-like surface at all.

Small parts of the Fermi surface of Zn have been most thoroughly investigated under pressure.

The influence of pressure on the extremal intersection S_1 of the "needle" of Zn with the plane perpendicular to the hexagonal axis was investigated by many authors, namely, by Dmitrenko, Verkin, and Lazarev[31] with the aid of the ice technique (p = 1700 bar), by Balain et al.[6] (p up to 25 bar), by Gaĭdukov and Itskevich[32] (p up to 8 kbar), by Itskevich, Voronovskiĭ, and Sukhoparov[33] (p up to 16 kbar), by Schirber and O'Sullivan[17,34] (p up to 5 kbar), and by Lazarus and Melz[35] (p up to 5 kbar). In these investigations they measured the de Haas–van Alphen or the Shubnikov–de Haas effects under pressure.

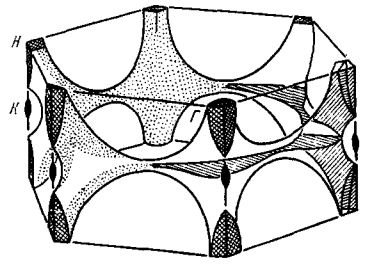

FIG. 9. Hole part of the Fermi surface of Zn in the first and second bands and the electron surfaces ("needles") in the third band [34]. The "needles" are the black ellipsoids around the points K of the hexagonal Brillouin zone.

*The Fermi surface of indium differs in some details from the Fermi surface of aluminum, but the sections considered here are identical for both metals.

The investigations have shown that the section S_1 of the "needle" increases rapidly upon compression, becoming seven times larger at $p \approx 16$ kbar[33].

A study was also made in[34] of the temperature dependence of the amplitudes of the de Haas–van Alphen oscillations connected with the "needle" and made it possible to calculate the pressure dependence of the effective mass corresponding to the section S_1.

In addition to the "needle," the Fermi surface of zinc has two other small sections. These are the minimal sections S_2 and S_3 of the horizontal and diagonal "arms," respectively, of the hole surface of the second band—of the so-called "monster."

O'Sullivan and Schirber[34] measured the influence of pressures up to 4 kbar on the de Haas–van Alphen oscillations corresponding to the sections S_1, S_2, and S_3. In analogy with the "needle," the section S_2 increases upon compression, but much more slowly. The section S_3, unlike the former two, becomes smaller under pressure.

The observed change, like the initial value of the area at atmospheric pressure, is sufficiently well described by the AFEM only for one section, S_3. For the section S_2, the AFEM gives approximately ten times the initial value from experiment, but describes satisfactorily the variation of the section under the influence of pressure.

For S_1, agreement between the initial value of the section obtained from experiment and the calculated one was attained by using the three-wave approximation. It is also possible to describe the observed change of S_1 in the same approximation. The principal part of the change is determined in this case by the decrease of the ratio c/a as a result of the compressibility anisotropy. All the results are listed in Table III.

The equal-energy surface of cadmium differs from that of zinc in the absence of a needle-like part of the Fermi surface and a break in the horizontal arms of the "monster" (Fig. 10). Since the ratio c/a for cadmium decreases under pressure and approaches the value of c/a for zinc, it becomes possible to observe the realignment of the Fermi surface of cadmium under hydrostatic compression. The use of pressures up to 16 kbar has enabled Itskevich and Voronovskiĭ[36] to observe qualitative changes in the angular dependence of the resistivity of Cd in fields ~14 kOe, which are attributed to the change of the topology of the Fermi surface and to the occurrence of open trajectories in the (0001) plane.

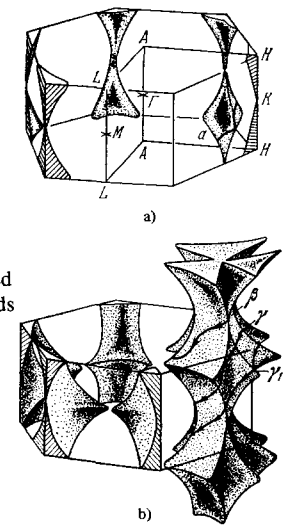

FIG. 10. Fermi surface of cadmium [38]. a) Sections of the hole part of the Fermi surface of the first band; b) hole surface of the second band in the reduced band and in the scheme of repeated bands (on the right).

A calculation carried out in the 3-OPW model also shows that at a pressure of ~15 kbar there should appear both a needle-like surface and connectivity of the "monster."

Schirber and O'Sullivan[37] investigated the influence of pressures up to 25 bar on the phase shift in the de Haas–van Alphen effect and obtained the values of $d(\ln S_i)/dp$ for the minimum (S_β) and maximum (S_γ) sections [by the (0001) plane] of the complicated open hole surface made up of the open parts of the "monster" and shown in Fig. 10 in the repeated-band scheme:

$$\frac{d\ln S_\beta}{dp} = (-9 \pm 1)\cdot 10^{-3}\ \text{kbar}^{-1}$$

and

$$\frac{d\ln S_\gamma}{dp} = (1 \pm 0.5)\cdot 10^{-3}\ \text{kbar}^{-1}.$$

The obtained sign of the change of the section S_γ under pressure agrees with the conclusion that the connectivity of the "monster" is restored under pressure.

The influence of pressures up to 25 bar on the maximum intersection of the (0001) plane with the cap-like hole surface of the first band (S_α) (see Fig. 10) was investigated in the same study. In addition, a study was made of the influence of pressures up to 9 kbar (produced in solid helium) on the intersection $S_{\alpha'}$ of the same surface with a plane inclined 28.5° to the basal plane (Fig. 10):

Table III

Investigated part of Fermi surface	Direction of magnetic field	Change of effective mass $\frac{d\ln m^*}{dp}$, 10^{-3} kbar^{-1}	$\frac{d\ln S}{dp}$, 10^{-3} kbar^{-1} (experiment)	$\frac{d\ln S}{dp}$, 10^{-3} кбар$^{-1}$ (AFEM calculation)
"Needle" (section S_1)	[0001]	140 [34]	370 [33] 320 [34]	130
Horizontal "arms" of "monster" (section S_2)	[11$\bar{2}$0]	>20 [34]	39.4 [34]	28
Diagonal "arms" of "monster" (section S_3)	In (11$\bar{2}$0) plane at an angle 20° to [0001]		−12.7 [34]	−8

$\frac{d\ln S_\alpha}{dp} = (-10 \pm 1)\cdot 10^{-3}$ kbar^{-1}, $\frac{d\ln S_{\alpha'}}{dp} = (-9.4 \pm 0.8)\cdot 10^{-3}$ kbar^{-1}.

6.2. Beryllium

The Fermi surface of beryllium differs from that of other divalent metals with hexagonal lattice. It is simpler and consists of a hole "corona" and a dumbbell-shaped electronic "cigar," the axis of which is parallel to the direction of the hexagonal axis (Fig. 11). This surface was constructed by fitting the experimental data to the matrix elements corresponding to the nonlocal pseudopotential model[39]. The discrepancy between the values of all the main sections and the experimental data did not exceed 1% in such a fitting.

O'Sullivan and Schirber[40,41] observed under pressure a change in the small extremal sections S_α and $S_{\alpha'}$ of the "cigar" and of the sections S_γ and S_β corresponding to the minimum and maximum intersections of the "corona" with planes parallel to the hexagonal axis.

Table IV lists the average values of $d(\ln S_i)/dp$ obtained from measurements of the de Haas–van Alphen oscillation frequencies up to ~ 4 kbar in solid helium and determined from the phase shift of the oscillations by producing pressures up to 25 bar in liquid helium. According to these data, the maximum sections of the electron and hole parts of the Fermi surface of beryllium (S_γ and $S_{\alpha'}$) decrease under pressure, and the large sections (S_α and S_β) increase.

Beryllium has an almost ideal close packing and as a result an almost isotropic compressibility, which should lead, in accord with the AFEM, to an identical increase under pressure of all the sections of the Fermi surface, namely, $d(\ln S)/dp = 0.58 \times 10^{-3}$ kbar^{-1}.

It is seen that the AFEM does not describe the observed changes of the Fermi surface of beryllium. We note that a strong disparity between the model and the experiment exists already at normal pressure.

A theoretical calculation of the quantities $d(\ln S_i)/dp$ with the aid of a model pseudopotential reconciled with the experimental data for Be at atmospheric pressure has been carried out in[39]. Satisfactory agreement was obtained with the experimental results of[41] (see Table IV).

6.3. Thallium

Anderson, Schirber, and Stone investigated the influence of pressure on the Fermi surface of thallium[42]. They measured the de Haas–van Alphen effect under pressure up to 25 bar by the phase-shift method.

Thallium is trivalent, and, owing to its large atomic number, spin-orbit effects play an important role in it.

A model of the Fermi surface of thallium was proposed by Soven, who used for its construction the relativistic OPW formalism[43], and was confirmed experimentally by Priestley[44]. Its parts in the third (holes) and fourth (electrons) bands are shown in Fig. 12. Table V shows the experimental results. The designations of the orbits bounding the measured sections are given in Fig. 12.

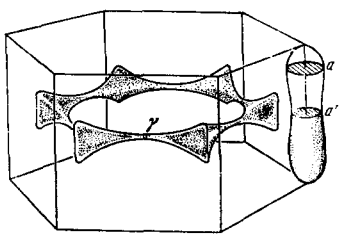

FIG. 11. Fermi surface of beryllium [41].

Table IV

Section	Direction of magnetic field	$\frac{d\ln S_i}{dp}$, 10^{-3} kbar^{-1} (experiment [41])	$\frac{d\ln S_i}{dp}$, 10^{-3} kbar^{-1} (calculation [39])
S_γ	[11$\bar{2}$0]	−4.5±1.0	−1.5±1.2
S_α	[0001]	0.2±0.05	0.17±0.1
$S_{\alpha'}$	[0001]	−0.08±0.04	−0.19±0.1
S_β	[11$\bar{2}$0]	0.3±0.1	0.35±0.14

It is indicated in the paper that the values of the derivatives with respect to pressure for sections of the large surfaces in the third and fourth bands are approximately the same as those following from the AFEM calculation using data on the compressibility. As to the sections of the small surfaces, the pressure effect for them is larger by approximately one order of magnitude. For a detailed comparison with theory, the authors calculated the extremal sections of the Fermi surface by the pseudopotential method in the many-wave approximation their dependence on the parameters of the spin-orbit splitting and on the model potential of Heine-Abarenkov, Animalu, and also the pressure dependences of these parameters. These results were used to calculate the derivatives $d(\ln S_i)/dp$. The obtained values are listed in the "calculation" column of Table V. The agreement with the experimental data can be regarded as satisfactory. No calculations were performed for the lowest-frequency oscillations since the locations of the corresponding parts of the Fermi surface in the Brillouin zone have not been established.

From the difference between the measured values of $d(\ln S)/dp$ for the sections α_1 and α_2, an estimate was made of the derivative, with respect to pressure, of the energy gap Δ due to the spin-orbit splitting:

$$\frac{d\ln\Delta}{dp} \leqslant 6\cdot 10^{-3} \text{ kbar}^{-1}.$$

7. SEMIMETALS

Bismuth, antimony, and arsenic crystallize in a rhombohedral structure with very close parameters, and the characters of their energy spectra are closely related. The lattice of a metal such as bismuth can be

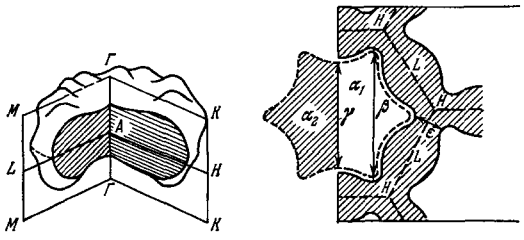

FIG. 12. Fermi surface of thallium. Left–hole surface in the third band, right–section of the electron surface of the fourth band by the plane AHL.

Table V

Section	Direction of magnetic field	$\frac{d \ln S_i}{dp}$, 10^{-3} kbar^{-1}, experiment	calculation
Third band central S_γ	[11$\bar{2}$0]	1.9±0.3	2.2
noncentral S_β	[11$\bar{2}$0]	1.9±0.3	
central S_{α_2}	[0001]	2.5±0.2	3.0
Fourth band non-central S_ε	[11$\bar{2}$0]	1.3±0.1	1.8
central S_{α_1}	[0001]	2.5±0.2	3
Fifth and sixth bands	[0001]	15±2	

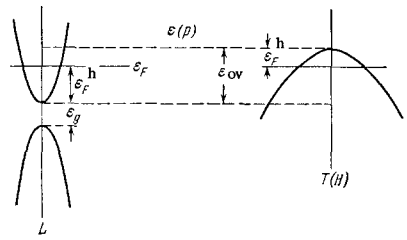

FIG. 13. Arrangement of electron and hole extrema near the Fermi level of semimetals (the hole extremum of Sb and As lies at H near the point T of the Brillouin zone).

obtained from the primitive cubic lattice by a small deformation, and is described by the lattice constant a, the rhombohedral angle α of the volume diagonal, and the parameter u characterizing the distance between the nearest atoms in the direction of the volume diagonal (Table VI).

The semimetallic properties of Bi, Sb, and As are due to the weak overlap of the fifth and sixth energy bands (Fig. 13), which leads to the occurrence of two small carrier groups of equal concentration—holes and electrons. Immediately adjacent to the semimetals, from the point of view of the electronic properties, is the group-IV element graphite. In analogy with Bi, Sb, and As, the conductivity in graphite is effected by small groups of holes and electrons of equal concentrations.

The smallness of the band overlap causes a small change of the lattice parameters under pressure to result in relatively large changes in the structure of the energy spectrum of the carriers and in all the properties of semimetals.

The fact that the equal-energy surfaces of Bi, Sb, As, and graphite are relatively close to ellipsoidal makes it possible to use for the investigation of the changes of the energy spectrum under pressure, in addition to quantum effects, also integral methods such as the measurement of the galvanomagnetic tensor in weak fields and the method proposed by Pospelov to determine the relative change of the carrier density, based on the measurements of the transverse magnetoresistance in strong magnetic fields[45]. In this method, to determine the dependence of the concentration on the pressure, use is made of the relation

$$\frac{\int_0^\infty \sigma_{xx}^p(H)\,dH}{\int_0^\infty \sigma_{xx}^0(H)\,dH} \approx \frac{N(p)}{N(0)}, \qquad (14)$$

where σ_{xx} is the conductivity in the basal plane of the crystal and $N = n_e = n_h$ is the carrier density. The method has the advantage that it does not require perfection of the single crystals and therefore makes it possible to carry out measurements at high quasihydrostatic pressures. As shown by the measurements of Brandt and Minima[16,46], the accuracy with which the carrier density is determined by this method is comparable with the accuracy of data obtained by oscillatory methods.

Table VI

	a, Å	α	u	$n_e = n_h$, cm^{-3}
Cube	—	60°	0.25	—
Bi	4.7459	57°14′	0.237	$2.8 \cdot 10^{17}$
Sb	4.50661	57°6,5′	0.233	$5.4 \cdot 10^{19}$
As	4.131	54°10′	0.226	$2.1 \cdot 10^{20}$

7.1. Bismuth

The Fermi surface of Bi consists of one hole ellipsoid of revolution at the point T of the Brillouin zone and three strongly anisotropic triaxial electron ellipsoids at the points L, inclined ~ 6° to the basal plane (Fig. 14). The dispersion law of the holes is quadratic in first approximation, while that of the electrons is not quadratic and is satisfactorily described by the Lax-Cohen model[47,48].

The influence of pressure on the oscillatory effects of bismuth was investigated in a large number of studies. The most complete data, obtained by Brandt and Itskevich with co-workers[49-52] at pressures up to 15 kbar, have shown that under pressure the electron and hole "ellipsoids" decrease in volume without significantly changing their anisotropy, and that the inclination of the "ellipsoids" to the basal plane remains constant within 5—10% in the indicated pressure region. The change of the extremal sections under pressure is shown in Fig. 15. The decrease of the carrier density of Bi under pressure, by approximately a factor of 5 at $p \approx 15$ kbar, is connected with the change in the overlap $\mathcal{E}_{ov}$ of the electron and hole extrema at the points L and T. The rate of change of the overlap under pressure, in accordance with the data of the galvanomagnetic

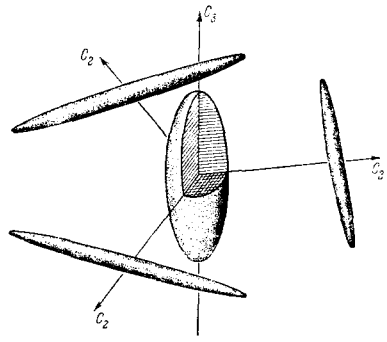

FIG. 14. Fermi surface of bismuth relative to the crystallographic axes. C_2 and C_3—binary and tragonal axes, respectively.

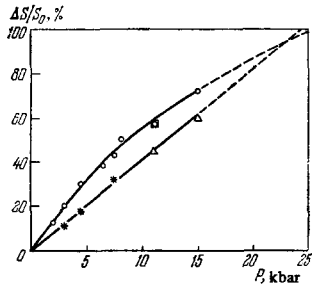

FIG. 15. Relative change under pressure of small sections of electron (○) and hole (∗, △) ellipsoids in Bi. □–large hole sections [51].

and oscillatory measurements, is $\partial \mathcal{E}_{ov}/\partial p = -1.4 \times 10^{-3}$ eV-kbar^{-1}[15,53]. One should expect the overlap to disappear completely in the region 25–26 kbar and Bi to change from the metallic to the dielectric state[51,54]. This assumption was confirmed by an investigation of the oscillatory and galvanomagnetic effects of Bi-Sb alloys, in which the initial overlap can be made much lower than in bismuth, and the metal-dielectric transition is clearly observed at pressures up to 20 kbar[15,53].

Measurements of the effective masses have shown[52] that the hole masses remain practically unchanged under compression, while the electron masses decrease greatly (by ~40% at p = 8 kbar), owing to the nonquadratic dispersion law of the electrons.

In the presence of overlap, it is very difficult to establish reliably the character of motion under pressure of the deeper extrema of the valence band and of the conduction band of bismuth. An answer to this question is obtained by investigating Bi-Sb alloys in the region where the overlap vanishes. On the basis of these investigations it was established that the energy gap $\mathcal{E}_h$ of Bi increases at a rate $\partial \mathcal{E}_h/\partial p \approx 1 \times 10^{-3}$ kbar^{-1}[53,55].

The general character of the motion of the extrema under the influence of pressure is shown in Fig. 16.

7.2. Antimony, Arsenic

The equal-energy surfaces of Sb and As are quite similar and consist of three curved electron "ellipsoids" at the points L of the Brillouin zone and of six even more curved hole "ellipsoids" near the point T. The hole "ellipsoids" of Sb are isolated from one another, and those of As are connected by long narrow necks and form a single multiply-connected surface[56,57] (Fig. 17). It is assumed that the lower

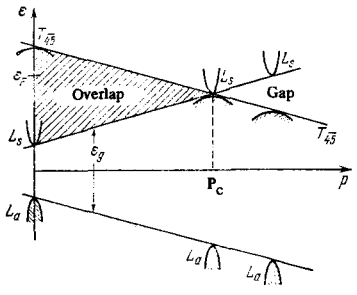

FIG. 16. Motion of extrema of bismuth under pressure [53]. p_c–pressure at which the band overlap vanishes and a transition takes place from the metallic to the superconducting state.

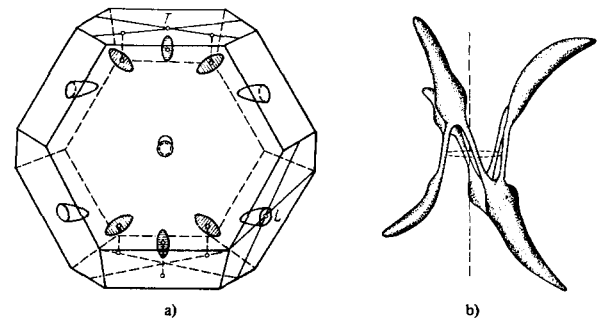

FIG. 17. a) Arrangement of hole (shaded) and electron "ellipsoids" of Sb in the reduced Brillouin zone [58]; b) multiply-connected hole Fermi surface of arsenic [59].

concentration of the carriers and the absence of necks in the hole surface of Sb are due to the larger spin-orbit interaction[57].

The Pospelov method was used to determine the general character of the change of the energy spectrum of these metals under pressure[45]. Brandt, Minima, and Pospelov[60,61] have established that in antimony, unlike in bismuth, the carrier density (and consequently also the band overlap $\mathcal{E}_{ov}$) grows under pressure, and increases by approximately 80% at p = 40 kbar. For antimony, as for bismuth, a decrease of the carrier density is observed (by approximately 40% at p = 30 kbar).

An investigation of the Shubnikov–de Haas effect in antimony under pressure was carried out by Minomura up to 4 kbar[62], and also by Minima and Lavrova in the interval 9–14 kbar[16]. It was observed that the hole "ellipsoid" of the Fermi surface of Sb increases under pressure similar to itself in first approximation, while its angle of inclination to the basal plane remains unchanged. The effective hole masses, in accordance with[16], increase strongly under pressure (by approximately 20% at p = 12 kbar).

The influence of a pressure up to 2–3 kbar on the phase of the de Haas–van Alphen oscillations of antimony was investigated by Schirber and O'Sullivan[63] and also by Priestly and Tay[64]. In these investigations, a small decrease of the minimum section of the hole "ellipsoid" S^g_{min} was observed. According to Schirber (communicated in a discussion of[64]), S^g_{min} decreases up to a pressure p ≈ 3 kbar, passes through a minimum, and then again increases in accordance with[16].

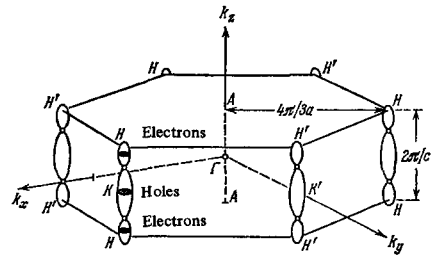

FIG. 18. Arrangement of electron and hole Fermi surfaces of graphite in the Brillouin zone [68].

7.3. Graphite

The electronic spectrum of graphite is usually described by the Slonczewski-Weiss model (SW)[65]. According to this model, the Fermi surface of graphite occupies a small part of the Brillouin zone (the carrier density is 3.34×10^{18} cm^{-3} at 4.2°K), is located along the vertical edges of the zone and is due to the small interaction of the conduction electrons of different layers. The SW model was verified in a number of experiments.

Figure 18 shows the Fermi surface of graphite. It consists of three cavities of ellipsoidal type—a large one in the middle and two smaller ones on the edges (the so-called majority carriers)*. In addition, carriers are also contained in small "pockets" near the hexagonal faces of the Brillouin zone.

From x-ray diffraction measurements made up to 16 kbar[66] it is known that the compressibility of graphite in the basal plane is negligible compared with the change of the distance between layers. Therefore the action of the pressure on graphite in this pressure interval is considered practically as unilateral compression and account is taken of the change of only those spectrum parameters which depend on the distance between layers.

The maximal sections S_{extr} of the Fermi surface of graphite by planes parallel to (0001) are connected in the SW model with the main parameters of the spectrum, γ_0, γ_1, and γ_2, which characterize respectively the interaction energies of the electrons of neighboring atoms within a layer, in neighboring layers, and in every other layer, and with the parameter Δ, which is connected with the nonequivalence of the neighboring atoms in a layer. If we neglect in the SW dispersion law the terms of higher order of smallness, then we get for the majority carriers of both signs $S_{extr} \sim |\gamma_1\gamma_2|/\gamma_0^2$, a Fermi energy $\mathcal{E}_F = 4\gamma_2/3$, and a cyclotron effective mass $m^* \sim \gamma_1/\gamma_0^2$. The influence of the pressure on the Fermi surface of graphite was investigated in two ways, by studying the oscillatory effects and by determining the integral galvanomagnetic characteristics.

Investigations of the oscillatory properties that have been carried out by Itskevich and Fisher up to 8 kbar[67], and also by Anderson, O'Sullivan, and Schirber up to 4 kbar[68], have shown that S_{extr} increases under pressure for the majority and minority carriers (Table VII), and that this increase is much larger than the compressibility, which amounts to 2.5×10^{-3} kbar^{-1} [see (8)]. It follows therefore that the interaction of the conduction electrons of different layers is very sensitive to the distance between layers.

The obtained data were used to calculate the dependence of the product $|\gamma_1\gamma_2|$ on the pressure under the assumption that γ_0 is independent of the pressure[66]. Data on the pressure dependence of $|\gamma_1\gamma_2|$ were confirmed by the galvanomagnetic measurements of Kechin, Likhter, and Stepanov[69].

Table VII

Carriers	$\frac{d \ln S}{dp}$, 10^3 kbar^{-1} (experiment)	$\frac{d \ln S}{dp}$, 10^3 kbar^{-1} (calculation)	Pressure interval
Majority holes	39 [67] 34 [68]		0—8 kbar
Majority electrons	40 [68]		0—4 kbar
Minority carriers	60 [68]	72	0—4 kbar

Arkhipov, Kechin, Likhter, and Pospelov[70] have shown that at high temperatures the effective mass $m^* \sim \gamma_1/\gamma_0^2$ is determined by the dependence of the electric resistance in the (0001) plane on the magnetic field directed along the hexagonal axis. By measuring this resistance, they determined the pressure dependence of γ_1 up to 9 kbar.

Anderson et al.[68] used a higher degree of approximation in the SW dispersion law, and calculated from the data for the majority carriers the proposed change of S_{extr} of the minority carriers (Table VII). They obtained sufficiently satisfactory agreement with experiment.

From the data of the oscillatory and galvanomagnetic measurements it is possible to calculate the pressure dependence of the parameters of the SW spectrum. In Table VIII are gathered the values obtained from these experiments for the logarithmic derivatives with respect to pressure for the main parameters of the spectrum: γ_1, γ_2, Δ, and E_F. The same table lists the estimated values of $d(\ln\gamma_4)/dp$ obtained by Kechin[71] (γ_4—the SW spectrum parameter corresponding to the interaction of the electrons of nonequivalent atoms in neighboring layers).

8. CHANGES OF FERMI SURFACES OF METALS UNDER UNILATERAL DEFORMATION

Unlike hydrostatic compression, unilateral deformation—compression or tension—can lead to a change in the symmetry of the crystal lattice (for example, when a cubic crystal is compressed along one of the crystallographic axes), and to a generally more complicated character of the variation of the Fermi surfaces.

At the present time, there exist data on the influence of unilateral deformations on the Fermi surfaces of copper, gold, silver,[72], white tin[73], zinc[74], and bismuth[75].

Table VIII

Spectrum parameters	$\frac{d \ln x}{dp}$, kbar^{-1}
$\gamma_1\gamma_2$	0,039 [67]
γ_1	0,020 [70]
γ_2	0,019 [67]
$\mathcal{E}_F$	0,019 [67]
Δ	0,09 [68]
γ_4	0,008 [71]

*Recently different points of view have been expressed in the literature concerning the signs of the carriers in the different parts of the Fermi surface of graphite. In the present review we adhere to the opinion prevalent to date, that holes are situated in the central part and electrons at the edges. This does not in any way affect the analysis that follows.

Table IX

Metal	Direction of magnetic field	Investigated part of the Fermi surface	$\frac{d \ln S_{extr}}{d \ln S_F}$	$\frac{d \ln S_{extr}}{d \ln \sigma}$, 10^{-3} kbar^{-1}
Cu	[100]	"Sphere"	2.4±0.5	−0.38±0.08
	[100]	"Rosette"	−2.1±0.8	0.33±0.13
	[111]	"Sphere"	0.6±0.2	−0.09±0.03
	[111]	"Neck"	−44±10	6.9±1.5
Ag	[100]	"Sphere"	2.2±0.3	−0.45±0.06
	[100]	"Rosette"	−2.4±0.5	0.49±0.1
	[111]	"Sphere"	0.8±0.3	−0.16±0.06
	[111]	"Neck"	−72±5	15±1
Au	[100]	"Sphere"	8±1	−1.0±0.1
	[100]	"Rosette"	4.0±1.0	−0.49±0.12
	[111]	"Sphere"	2.6±0.4	−0.32±0.05
	[111]	"Neck"	−60±8	7.4±1.2

Investigations of the de Haas–van Alphen effect under uniaxial elastic tension σ of unrestrained samples of copper, silver, and gold up to 100–150 kg/cm^2 along the axes [100] and [111] have revealed[72] that, unlike hydrostatic compression, the changes of the cross sections of the "sphere" and of the "neck" have opposite signs: the cross section of the "neck" is strongly increased by tension, whereas the cross sections of the "sphere" decrease (Table IX). The distortions of the Fermi surface greatly exceed in this case those observed under hydrostatic compression. Thus, the value of $d(\ln S_2)/d(\ln S_F)$ for the "neck" under tension amounts to −44 for Cu, −72 for Ag, and −60 for Au. The change of the cross sections of the "sphere," although of the same sign as the change of the volume of the Fermi sphere of the free electrons, is quantitatively in worse agreement with the AFEM description than under hydrostatic compression (see Tables IX and I).

A study of the influence of unilateral compression on the de Haas–van Alphen effect in bismuth[75] has shown that under a load of ~ 350 kg/cm^2, applied along the [111] axis, the relative decrease of the cross sections of the electron ellipsoids is ~ 5%, which is approximately 2.5 times larger than the effect observed under unilateral compression at 350 bar.

For zinc, which has an anisotropic compressibility, the change of the minimum cross section S_{min} of the "needle" under a small compressive load (~100 kg/cm^2) along the [0001] axis reaches ~ (4–5)%[74]. Under hydrostatic compression of 100 bar, this value is 3.5% (see Table III). The fact that the difference between the effects of hydrostatic compression and unilateral compression along the [0001] axis is much smaller than for bismuth and is a consequence of the anomalously large compressibility of the zinc along this axis, as a result of which the changes in the volume and shape of the Brillouin zone are close to each other in both cases.

In tin stretched along the [001] axis, an increase is observed in the frequency of de Haas–van Alphen oscillations corresponding to the minimum section of the hole surface in the third band, the relative magnitude of which is ~0.01 kg/cm^2[73]. Comparison with effects of hydrostatic compression in the case of tin is impossible, owing to the lack of experimental data. On the basis of the presented (albeit very limited) experimental material it can be concluded that the unique change of the lattice under unilateral deformation uncovers additional possibilities for investigating its role in the formation of the energy spectrum of metals. However, the limiting magnitude of the uniaxial deformations is limited, unfortunately, by the small forces, the values of which are determined by the elastic limit of the sample.

Under loads exceeding the elastic limit, irreversible changes result from plastic deformation. Therefore, even though the derivative $d(\ln S)/d\sigma$ is larger than in hydrostatic compression, the maximum value of the observed effects does not exceed 4–5%.

9. CONCLUSION

The foregoing review of the experimental work shows that at the contemporary level of technology of obtaining high and sufficiently hydrostatic pressures at low temperatures, the study of oscillatory effects under conditions of hydrostatic compression is perfectly feasible and requires no special or expensive installations.

The main progress in these investigations has been reached because of two methodological accomplishments: the development of methods for maintaining constant the pressure generated at temperatures above the experimental temperature, when the medium transmitting the pressure to the sample is still sufficiently plastic, and the use of the phase-shift method to register small changes in the oscillation frequency, making it possible to carry out investigations at the low pressures produced by liquid helium. The first of these accomplishments has uncovered the possibility of obtaining pressures that are hydrostatic to a sufficient degree, reaching about 20 kbar, which in many cases suffices to extract essentially important information.

Further increase of the range of hydrostatic pressures at low temperatures will apparently entail the use of liquids with low solidification temperatures, such as pentane or isopentane. In addition, this will require the use of special nonmagnetic steels having high strength characteristics. One can hope that in the near future this method will yield pressures that are suitable for the investigation of oscillatory effects and exceed 30 kbar.

The presently known experimental data indicate that the AFEM gives qualitatively correct information on the

character and magnitude of the change under pressure of large principal sections of the Fermi surface. For small sections, an important role in the pressure effect is played by the change of the lattice potential. The use of the many-wave approximation in this case greatly improves the agreement with experiment, but calls for allowance for the pressure dependence of the form factor, something not always possible when the existing models are used. Experiments under pressure permit a choice of the best approximation for the description of the real Fermi surface of the metal, since the changes that occur under pressure in the electron spectrum are very sensitive to the choice of the initial approximation.

An interesting trend in the study of the electronic properties of metals under pressure is the investigation of specific "electronic" phase transitions connected with the change of the topology of the Fermi surface and with the vanishing and appearance of new cavities in this surface. It is obvious that to observe such effects in a large number of metals it is necessary to have much higher pressures than hitherto attained. In many cases, however, for example in CdZn and in Bi-Sb alloys, it is possible to observe transitions of this type already in existing experimental conditions, making it possible to obtain additional information on the structure of the energy spectrum.

Considerable interest may also attach to investigations of the combined action of pressure, impurities, and of magnetic and strong electric fields on the properties of matter at low and infralow temperatures.

The methods developed for the production of high pressures at low temperatures also make it possible to study under pressure other branches of the quasiparticle spectrum in the metal. Reports have been published of investigations, under pressure, of the energy gap in superconductors and of its anisotropy, of the phonon spectrum, etc.

In conclusion, we wish to point out the prospects of investigating the electron spectrum of metals under conditions of unilateral deformation, since unilateral deformation makes it possible to change not only the interatomic distances but also the symmetry of crystals.

The authors are grateful to V. F. Gantmakher for useful remarks made after reading the manuscript.

[1] E. O. Kane, J. Phys. Chem. Solids 1, 249 (1957).
[2] B. T. Geĭlikman and V. Kresin, Fiz. Tverd. Tela 7, 3294 (1965) [Sov. Phys.-Solid State 7, 2659 (1966)].
[3] I. M. Lifshitz, Zh. Eksp. Teor. Fiz. 38, 1569 (1960) [Sov. Phys.-JETP 11, 1130 (1960)].
[4] I. M. Lifshitz and M. I. Kaganov, Usp. Fiz. Nauk 78, 411 (1962); 87, 389 (1965) [Sov. Phys.-Uspekhi 5, 878 (1963); 8, 805 (1966)].
[5] J. S. Dugdale, Some Aspects of High Pressures at Low Temperatures in "Advances in High Pressures Research", ed. by R. S. Bradley, New York—London, Acad. Press, 1969.
[6] K. S. Balain, C. G. Grenier and J. M. Reynolds, Phys. Rev. 119, 935 (1960).
[7] J. M. Templeton, Proc. Roy. Soc. A292, (No. 1430), 413 (1966).
[8] D. Shoenberg and P. J. Stiles, Proc. Roy. Soc. A281, 62 (1964).
[9] B. G. Lazarev and L. S. Kan, Zh. Eksp. Teor. Fiz. 14, 470 (1944).
[10] N. B. Brandt and A. K. Tomashchik, Pribory i Tekhn. Éksperim. No. 2, 113 (1958).
[11] E. S. Itskevich, Zh. Eksp. Teor. Fiz. 42, 1173 (1962) [Sov. Phys.-JETP 15, 811 (1962)]; Pribory i Tekhn. Eksperim. No. 4, 148 (1963).
[12] E. S. Itskevich, A. N. Voronovskiĭ, A. F. Gavrilov and V. A. Sukhoparov, Pribory i Tekhn. Eksperim. No. 6, 161 (1966).
[13] E. S. Itskevich, V. F. Kraĭdenov, Z. A. Mironova, E. L. Slavyaninova, V. A. Sukhoparov, ibid. No. 1, 187 (1968).
[14] N. E. Alekseevskiĭ, N. B. Brandt and T. I. Kostina, Izv. Akad. Nauk SSSR, Ser. Fiz. 16(3), 233 (1952).
[15] N. B. Brandt and Ya. G. Ponomarev, Zh. Eksp. Teor. Fiz. 55, 1215 (1968) [Sov. Phys.-JETP 28, 635 (1969)].
[16] N. Ya. Minina and V. V. Lavrova, ibid. 57, 354 (1969) [30, 194 (1970)].
[17] J. E. Schirber, Phys. Rev. 140, A265 (1965).
[18] C. H. Hinrichs and C. A. Swenson, Phys. Rev. 123, 1106 (1961); J. E. Schirber and C. A. Swenson, Phys. Rev. 123, 1115 (1961).
[19] J. S. Dugdale and J. A. Hulbert, Can. J. Phys. 35, 720 (1957); Cf. also: C. Swenson, High Pressure Physics (Russ. transl.) IL, 1963, p. 36.
[20] W. A. Harrison, Pseudopotentials in the Theory of Metals, Benjamin, 1966.
[21] W. J. O'Sullivan and J. E. Schirber, Phys. Rev. 170, (3), 667 (1968).
[22] Harold L. Davis, J. S. Faulkner and H. W. Joy, Phys. Rev. 167, 601 (1968).
[23] J. R. Anderson, W. J. O'Sullivan and J. E. Schirber, Phys. Rev. 153(3), 721 (1967); Bull. Amer. Phys. Soc. 13, 508 (1968).
[24] J. R. Anderson and A. V. Gold, Phys. Rev. 139, 1459 (1965).
[25] R. Glinski and J. M. Templeton, J. Low Temp. Phys. 1, (3), 223 (1969).
[26] G. M. Beardsley and A. T. Stewart, Bull. Amer. Phys. Soc. 14, (4), 576 (1969).
[27] J. J. Vuillemin and H. J. Bryant, Phys. Rev. Letts. 23(18), 914 (1969).
[28] Peter J. Melz, Phys. Rev. 152, 540 (1966).
[29] W. A. Harrison, Phys. Rev. 118, 1182 (1960).
[30] W. J. O'Sullivan and J. E. Schirber, Solid State Comm. 5, 525 (1967).
[31] I. M. Dmitrenko, B. I. Verkin and B. G. Lazarev, Zh. Eksp. Teor. Fiz. 35, 328 (1959) [Sov. Phys.-JETP 8, 229 (1959)].
[32] Yu. P. Gaĭdukov and E. S. Itskevich, ibid. 45, 71 (1963) [18, 51 (1964)].
[33] E. S. Itskevich, A. N. Voronovskiĭ and V. A. Sukhoparov, ZhETF Pis. Red. 2, 67 (1965) [JETP Lett. 2, 42 (1965)].
[34] W. J. O'Sullivan and J. E. Schirber, Phys. Rev. 151, 484 (1966).
[35] D. Lasarus and P. J. Melz, Bull. Amer. Phys. Soc. 11(2), 169 (1966).
[36] E. S. Itskevich and A. N. Voronovskiĭ, ZhETF Pis. Red. 4(6), 226 (1966) [JETP Lett. 4, 154 (1966)].

[37] J. E. Schirber and W. J. O'Sullivan, Eleventh Intern. Conf. on Low Temperature Physics, St. Andrews, 1968, vol. 2, p. 1141 (1968).
[38] D. C. Tsui and R. W. Stark, Phys. Rev. Letts. 16 (1), 19 (1966).
[39] J. H. Tripp, P. M. Everett, W. L. Gordon and R. W. Stark, Phys. Rev. 180, 669 (1969).
[40] W. J. O'Sullivan and J. E. Schirber, Phys. Letts. A25 (2), 124 (1967).
[41] J. E. Schirber and W. J. O'Sullivan, Phys. Rev. 184 (3), 628 (1969).
[42] J. R. Anderson, J. E. Schirber and D. R. Stone, Actes du Colloque international du CNRS sur les propriétés physiques des solides sous pression, Grénoble (1969).
[43] P. Soven, Phys. Rev. 137, A1706 (1965).
[44] M. G. Priestley, Phys. Rev. 148, 580 (1966).
[45] Yu. A. Pospelov, Fiz. Tverd. Tela 9, 589 (1967) [Sov. Phys.-Solid State 9, 451 (1967)].
[46] N. B. Brandt, N. Ya. Minina, Yu. A. Pospelov, ibid. 10, 1268 (1968) [10, 1011 (1968)].
[47] B. Lax, Phys. Rev. 129, 2055 (1963).
[48] M. H. Cohen, Phys. Rev. 121, 387 (1961).
[49] N. B. Brandt and V. A. Venttsel', Zh. Eksp. Teor. Fiz. 35, 1083 (1958) [Sov. Phys.-JETP 8, 757 (1959)].
[50] N. B. Brandt, Yu. P. Gaĭdukov, E. S. Itskevich and N. Ya. Minina, ibid. 47, 455 (1964) [20, 301 (1965)].
[51] E. S. Itskevich and L. M. Fisher, ibid. 53, 98 (1967) [26, 66 (1968)].
[52] E. S. Itskevich and L. M. Fisher, ibid. 53, 1885 (1967) [26, 1072 (1968)].
[53] N. B. Brandt and S. M. Chudinov, ibid. 59, 1494 (1970) [32, 815 (1971)].
[54] D. Balla and N. B. Brandt, ibid. 47, 1653 (1964) [20, 1111 (1965)].
[55] N. B. Brandt, Kh. Dittman, Ya. G. Ponomarev and S. M. Chudinov, ZhETF Pis. Red. 11, 250 (1970) [JETP Lett. 11, 160 (1970)].
[56] L. R. Windmiller, Phys. Rev. 149, A472 (1966).
[57] M. G. Priestley, L. R. Windmiller, J. B. Ketterson and Y. Eckstein, Phys. Rev. 154, 671 (1967).
[58] N. B. Brandt, N. Ya. Minina and Chou Chen-kang, Zh. Eksp. Teor. Fiz. 51, 108 (1966) [Sov. Phys.-JETP 24, 73 (1967)].
[59] P. J. Lin and L. M. Falikov, Phys. Rev. 142, 441 (1966).
[60] N. B. Brandt and N. Ya. Minina, ZhETF Pis. Red. 7, 264 (1968) [JETP Lett. 7, 205 (1968)].
[61] N. B. Brandt, N. Ya. Minina and Yu. A. Pospelov, Zh. Eksp. Teor. Fiz. 55, 1656 (1968) [Sov. Phys.-JETP 28, 869 (1969)].
[62] S. Minomura, S. Tanuma, G. Fuji, M. Nishizawa and H. Nagano, Phys. Letts. 29A (1), 16 (1969).
[63] J. E. Schirber and W. J. O'Sullivan, Solid State Comm. 7, 709 (1969).
[64] M. G. Priestley and C. Y. Tay, Actes du Colloque international du CNRS sur les propriétés physiques des solides sous pression, Grénoble (1969).
[65] I. S. Slonczewski and P. R. Weiss, Phys. Rev. 109, 272 (1958).
[66] S. S. Kabalkina and L. F. Vereshchagin, Dokl. Akad. Nauk SSSR 131,300(1960)[Sov.Phys.-Doklady 5,373(1960)].
[67] E. S. Itskevich and L. M. Fisher, ZhETF Pis. Red. 5, 141 (1967) [JETP Lett. 5, 114 (1967)].
[68] J. R. Anderson, W. J. O'Sullivan, J. E. Schirber and D. E. Soule, Phys. Rev. 164, 1038 (1967).
[69] V. V. Kechin, A. I. Likhter and G. N. Stepanov, Fiz. Tverd. Tela 10, 1242 (1968) [Sov. Phys.-Solid State 10, 987 (1968)].
[70] R. G. Arkhipov, V. V. Kechin, A. I. Likhter and Yu. A. Pospelov, Zh. Eksp. Teor. Fiz. 44, 1964 (1963) [Sov. Phys.-JETP 17, 1321 (1963)].
[71] V. V. Kechin, Fiz. Tverd. Tela 11, 1788 (1969) [Sov. Phys.-Solid State 11, 1448 (1970)].
[72] D. Shoenberg and B. R. Watts, Phil. Mag. 15 (138), 1275 (1967).
[73] R. H. Hum and J. M. Perz, Phys. Letts. 28A (8), 575 (1969).
[74] B. I. Verkin and I. M. Dmitrenko, Zh. Eksp. Teor. Fiz. 35, 291 (1958) [Sov. Phys.-JETP 8, 200 (1959)].
[75] N. B. Brandt and G. A. Ryabenko, ibid. 37, 389 (1959) [10, 278 (1960)].

Translated by J. G. Adashko
37